Asensi-Fabado, A.; García-Breijo, F.; Reig Armiñana, J. (2010). Ozone-induced reductions in below-ground biomass: an anatomical approach in potato. Plant, Cell and Environment. 33(7):1070-1083. doi:10.1111/j.1365-3040.2010.02128.x.

Ozone-induced reductions in below-ground biomass: an anatomical approach in potato

AMPARO ASENSI-FABADO[1,2], FRANCISCO J. GARCÍA-BREIJO[2,3] & JOSÉ REIG-ARMIÑANA[2]

[1]Departamento de Biología Vegetal, Universitat de València, C/Doctor Moliner 50, 46100 Burjassot, Valencia, Spain, [2]Laboratorio de Anatomía e Histología Vegetal 'Julio Iranzo', Jardín Botánico, Universitat de València, C/Quart 80, 46008 Valencia, Spain, [3]Departamento de Ecosistemas Agroforestales, Escuela Técnica Superior del Medio Rural y Enología, Universidad Politécnica de Valencia, Avda. Blasco Ibáñez 21, 46010 Valencia, Spain

ABSTRACT

Potato plants were grown in open-top chambers under three ozone concentrations during two complete cropping seasons (93 and 77 d in 2004 and 2005, respectively). The effects of chronic exposure to ozone on leaf anatomy, cell ultrastructure and crop yield were studied. Severe cell damage was found, even at ambient ozone levels, mainly affecting the spongy parenchyma and areas near the stomata. Damage to the cell wall caused loss of cell contact, and loss of turgor pressure due to tonoplast disintegration, contributed to cell collapse. Phloem sieve plates were obstructed by callose accumulation, and damaged mesophyll cells increased their starch stores. Tuber yield fell sharply (24–44%), due to the biggest tubers becoming smaller, which affected commercial yield. These anatomical findings show the mechanisms of ozone effect on assimilate partitioning, and thus crop yield decrease, in potato. Further implications of ozone causing reductions in below-ground biomass are also discussed.

Key-words: assimilate partitioning; callose; crop yield; leaf anatomy; open-top chambers; ozone; potato; starch.

INTRODUCTION

Tropospheric ozone is considered the most important phytotoxic air pollutant worldwide (Krupa *et al*. 2001). Intercontinental transport of ozone and its precursors has been demonstrated (Derwent *et al*. 2004), which shows that ozone pollution is a *trans*- boundary problem. Mean global ozone concentration was 50 ppb in the year 2000 (Fiscus, Booker & Burkey 2005), and is growing due to the increase of anthropogenic precursors. The most pessimistic predictions suggest future average ozone concentrations of up to 80 ppb in the year 2100 (Prather *et al*. 2001; Vingarzan 2004). The southern part of Europe is affected by high ozone concentrations, especially the Mediterranean basin, which favours the formation and accumulation of this pollutant because of its particular conditions of high solar radiation and temperatures, as well as the re-circulation dynamics of its air masses (Millán *et al*. 2002). Ozone has a negative impact on forests and crops; a number of studies within the framework of the US National Crop Loss Assessment Network (Heagle 1989) and the more recent International Cooperative Program on Effects of Air Pollutants on Natural Vegetation and Crops (Kärenlampi & Skärby 1996) have shown that ozone causes a significant decrease in crop yield. The extent of crop loss depends on species or cultivar sensitivity, drought stress and other growth conditions. Ozone damage to crops has economic costs for society. In the United States, a general figure of 2.8–5.8 billion dollars (at 1990 values) as gains from reducing or eliminating ozone precursors from motor-vehicle emissions is acknowledged by the Environmental Protection Agency (U.S. EPA 2006). In Europe (specifically the Netherlands), reducing ozone to background levels of 20 ppb would benefit agriculture by 310 million euros, including a surprisingly large surplus in the cattle farming sector through yield increases on grassland (Kuik *et al*. 2000). The economic losses for four major grain crops in East Asia ranged from 0.24 to 3.5 billion U.S. dollars in 1990 and are expected to be 0.4–6.4 billion dollars in 2020, the highest losses affecting China (Wang & Mauzerall 2004). Ambient ozone concentrations in the Mediterranean region cause remarkable yield decreases in important crops such as wheat (20–27%), tomato (17–24%) or watermelon (19–39%) (Fumagalli *et al*. 2001). It should be noted that plant development in many crops occurs during high ozone periods (spring–summer).

Potato is a staple food, the fourth most important crop in the world after wheat, rice and maize (FAO 2009), and the second most important in Europe after wheat. It is of great importance in the human diet because of its harvest index (ratio of edible to non-edible components), which is much higher than in cereals. As for many plant species, ozone-sensitive and -tolerant cultivars have been reported for potato (Clarke, Greenhalgh-Weidman & Brennan 1990). Nevertheless, important yield reductions due to ambient ozone (14–31%) have been found in cvs. Dark Red Norland (Heagle, Miller & Pursley 2003) and Norchip (Clarke *et al.* 1990).

The causes of yield reduction by ozone seem to be multiple and are related to two main phenomena: (1) inhibition of photosynthesis, reflected in a decrease in carbon

Correspondence: A. Asensi-Fabado. Departamento de Biologia Vegetal, Universitat de Barcelona, Av. Diagonal 645, 08028 Barcelona, Spain. Fax: +34 934112842; e-mail: masensif@ub.edu

assimilation (Runeckles & Chevone 1992; Morgan, Ainsworth & Long 2003), degradation of Rubisco (Pell, Eckhardt & Eniyedi 1992) and photoinhibition (Carrasco-Rodríguez & Del Valle-Tascón 2001); and (2) changes in assimilate partitioning, which suggest an inhibition of assimilate translocation (Miller, Heagle & Pursley 1998; Grantz & Yang 2000; Guidi, Degl'Innocenti & Soldatini 2002). It is generally accepted that, at the biochemical level, ozone damage is mediated by reactive oxygen species (ROS). ROS, which are generated from ozone reactions in the apoplast, disrupt membrane integrity and pigment structure and oxidize proteins (Langebartels *et al.* 2002).

In contrast to the vast amount of physiological, biochemical and molecular data on ozone effects on plants, few studies have been made at the anatomical level using microscopy methods. Anatomical studies provide a holistic approach and permit differential location of particular responses at the cell/tissue level, therefore facilitating data integration that may lead to a better understanding of phenomena. In the research into ozone effects on plants, tissue anatomy has been mainly studied in forest species. New knowledge has emerged, such as the significance of the different displays of visible symptoms: bronzing or reddening, which consists of groups of palisade parenchyma cells accumulating proanthocyanidins or anthocyans, oxidized on a gradient according to the intensity of oxidative stress, especially in light-exposed areas of the leaves; and stippling, which reflects mesophyll cells undergoing hypersensitive response-like reactions (cell content disruption forming apoptotic-like bodies) (Günthardt-Goerg & Vollenweider 2007). Size reduction of chloroplasts and swelling of the thylakoids has been observed (Pääkkönen, Holopainen & Kärenlampi 1995; Günthardt-Goerg *et al.* 2000; Gravano *et al.* 2003, 2004; Oksanen *et al.* 2003), also in crop species (Miyake *et al.* 1989; Violini *et al.* 1992); even loss of thylakoid organization in grana has been found (Faoro & Iriti 2009). These effects constitute an anatomical basis for the inhibition of photosynthesis. Pectic protrusions and polyphenolic incrustations in cell walls indicate reactions to apoplastic ROS generated following ozone uptake (Günthardt-Goerg *et al.* 2000). Furthermore, these anatomical markers of the ozone effect have converted microscopy into a very useful and recommended complementary tool for validation of visible symptoms observed in the field.

Along with the previously mentioned similarities between species, there are also responses to ozone that are particular to groups of species, suggesting relationships with their physiological strategies. For example, damaged palisade cells collapse in broadleaved trees, whereas mesophyll cells in conifer needles apparently die without cell wall collapse, probably because they are more robust (Günthardt-Goerg & Vollenweider 2007). Another example of particular ozone responses is the thickening of the cuticle found in *Pistacia lentiscus* (Reig-Armiñana *et al.* 2004) and *Arbutus unedo* (Bussotti *et al.* 2003), both Mediterranean evergreen species. The cuticle response may be a mechanism in these species that is related to their drought-avoidance strategy. Though ozone effects have never been studied in potato at the anatomical level, potato is a fast-developing crop, which might display particular responses to ozone. In the present study, potato cv. Agria was used. This is a cultivar normally grown by farmers in the Valencia area that develops ozone-induced visible injuries when grown commercially in the field. The objectives of this study are to characterize the effects of chronic exposure to ozone on tuber yield and foliar anatomy of potato, in order to gain insight into the anatomical basis for crop yield decrease.

MATERIALS AND METHODS

Experimental site

The experiment was conducted at the Centro de Capacitación Agraria of the Generalitat Valenciana, located at Carcaixent. The site is a rural area 40 km south of the city of Valencia in eastern Spain (39°7′N, 0°27′W), 20 m above sea level. No major air pollution sources were located in the vicinity.

Plant material

Potato tubers (*Solanum tuberosum* L. var. Agria) were sown manually in 20 L-pots (one tuber per pot) in standard potting soil mix (Terraplant 1, BASF). Pots were placed inside nine open-top chambers (OTC). Plants developed inside the chambers until harvest (when the canopy had senesced to about 90% of its maximum), under the three treatments described below. There were three plants per chamber and three chambers per treatment, making nine plants per treatment. Plants were watered daily to field capacity by drip irrigation. Soil water potential was monitored with a tensiometer and maintained above –30 kPa (at 20 cm below the soil surface) to ensure that plants did not suffer water stress. In 2004, the crop was sown on 20 January, emerged on 16 February and was harvested on 18 May; in 2005, the crop was sown on 3 February, emerged on 4 March and was harvested on 19 May.

Leaf samples for microscopy were collected on 6 May 2004 and on 2 May 2005, when crops were at an advanced state of development (after 77–86% of their lifespan, about 1 week before the senescence of the oldest leaves), in order to study the damage resulting from prolonged ozone exposure. Samples taken in 2004 were used to study foliar anatomy and cell ultrastructure, and samples taken in 2005 were used for callose location and the study of starch content. One young leaflet and one mature leaflet (third leaflet from the second fully expanded leaf and third leaflet from the fifth fully expanded leaf, respectively, on a random shoot of the plant) were collected in each of two plants per chamber (six plants per treatment); leaflets of the same age were of similar size. Sampling was carried out at 1300 h in both years.

Ozone exposure

Three different ozone treatments were applied within the OTC from plant emergence until harvest (from 16 February

until 18 May 2004 and from 4 March until 19 May 2005): charcoal-filtered air (CF), in which approximately 80% ambient ozone was removed, ambient air passing a particle filter only (NF), and NF air plus 80–120 ppb of ozone following a sinusoidal profile (NF^+), for 5 h a day from Monday to Friday (0830–1330 h UTC). There were three chambers per treatment, distributed across the experimental site according to a fully-randomized design. The fumigation regime in the NF^+ treatments and the OTC facility are described in detail in Asensi-Fabado *et al.* (2008).

Ozone, sulphur dioxide and nitrogen oxides were monitored continuously throughout the experiments. The air sampling point was located at the centre of each chamber at a height of 1 m. Ozone was determined by UV absorbance (Dasibi mod. 1008 RS, Dasibi Environmental Corporation, Glendale, CA, USA), SO_2 by fluorescence (Dasibi mod. 4181) and nitrogen oxides by chemiluminescence (Dasibi mod. 2108).

Microscopy methods

Foliar anatomy and starch and callose histochemical location were studied in leaf sections by light/epifluorescence microscopy. Cell ultrastructure was determined by transmission electron microscopy.

Light and epifluorescence microscopy

Semi-thin cross-sections (1 μm thick) and 15-μm-thick sections were examined. The following protocol was used to obtain semi-thin sections: samples were fixed in a mixture of 5% glutaraldehyde and 5% paraformaldehyde buffered with 100 mM sodium phosphate, pH 7.2, for 10 h at 4 °C. After three washings in sodium phosphate buffer, samples were dehydrated in an increasing ethanol series. Then samples were embedded in LR-White medium-grade acrylic resin (London Resin Co., London, UK) in a mixture series of absolute ethanol and resin, this latter in an increasing proportion until pure resin. Semi-thin sections were obtained with a Sorvall MT-5000 ultramicrotome (Giraldi-Dupont, Wilmington, DE, USA) provided with a glass knife (45°) obtained from a special glass (Glass Strips Leica 6.4 mm) in a knifemaker (Reichert-Jung, Wien, Austria). Another set of leaf samples was washed in 100 mM sodium phosphate buffer, pH 7.2, for 1 h at 4 °C, then dehydrated in an ethanol series until 80% ethanol for fixation and preservation; 15-μm-thick sections were obtained from these samples with a freezing microtome (Leica CM1325). The following stains were used:

- Toluidine blue (1%) on 1-μm-thick sections for anatomical observations.
- Aniline blue (1%) on 15-μm-thick sections for callose location. Stained sections were observed immediately under an epifluorescence microscope with epifluorescent blue emission of 460–490 nm wavelength.
- Aqueous 1% iodine solution (Lugol) on semi-thin 1-μm-thick sections for starch location.

Samples were observed with an Olympus Provis AX 70 microscope and photographed with an Olympus Camedia C-2000 Z digital camera.

Transmission electron microscopy

Samples were fixed as described to obtain semi-thin sections. After three washings in sodium phosphate buffer, samples were post-fixed in buffered 2% OsO_4 for 2 h and subsequently washed with 100 mM sodium phosphate buffer, pH 7.2, for 15 min. Samples were then dehydrated in an increasing ethanol series and embedded in LR-White medium-grade acrylic resin (London Resin Co.), as detailed for semi-thin sections. Ultra-thin sections (70 nm-thick) were obtained with an Ultratome Nova LKB Bromma ultramicrotome provided with a DIATOME Ultra 45° diamond knife. Ultra-thin sections were stained with 2% lead citrate and 2% uranyl acetate for 10 min each, then observed with a JEOL JEM-1010 (100 kV) transmission electron microscope (Jeol Ltd., Tokyo, Japan); they were photographed with a MegaView III digital camera and AnalySIS image acquisition software provided by the Microscopy Service of Valencia University SCSIE.

Quantification of stomatal density

For each of three mature leaves per treatment, a 1×1 cm section was cut midway between the midrib and margin. The leaf sections were cleared with 5% sodium hypochlorite for 5 min, stained with safranin and fast green for another 5 min and washed with 96% ethanol. Stomata were counted under the light microscope at ×200 magnification on both upper and lower leaf surfaces, in five randomly selected fields per leaf surface for each leaf section.

Crop yield

Tubers were classified into commercial (size $\geq$ 40 mm) and non-commercial (size < 40 mm) tubers, according to Spanish legislation (Official State Gazette, BOE, no. 166, 13/7/1983). Individual tuber weights from each category were measured. To gather more information on the 2005 harvest, tuber size categories were increased: <30 mm, 30 mm–<40 mm, 40 mm–<60 mm, ≥60 mm. Size categories were determined using 30, 40 and 60 mm-side square meshes.

Statistics

Statistical analysis was performed with SPSS v12.0. Data sets were assessed for normality by means of the Kolmogorov-Smirnov test ($\alpha = 0.05$). Normal data were analysed with analysis of variance, followed by the least squares difference post-hoc test (group variance homogeneity was checked with the Levene test). A *t*-test for related samples compared stomatal density between the two leaf surfaces. Because non-normal data could not be improved adequately by transformation, mean comparison used the Kruskal-Wallis multiple test, followed by post-hoc pair

comparisons using the Mann-Whitney *U*-test. $P < 0.05$ were considered significant. Chamber-to-chamber variation within each treatment was analysed, and no significant differences were found.

RESULTS

Air quality, ozone exposure and visible injury

Daily, 12 h average concentrations of ozone between sunrise and sunset (0800–2000 h) in the three OTC treatments during the two growing seasons are shown in Fig. 1. The trend for ozone concentrations in the NF treatments was typically seasonal, with high values during solar radiation and warm periods. In particular, the 2005 period was characterized by fairly high background ozone concentration. Differences in ozone exposure between treatments were evident in the AOT40 (accumulated exposure over a threshold of 40 ppb between sunrise and sunset) values. The AOT40 exposure index for ozone was calculated for the period from plant emergence until harvest in the CF, NF and NF^+ treatments, resulting in 8, 2361 and 14 071 ppb h, respectively, in the 2004 season; and in 33, 4186 and 16 488 ppb h in the 2005 season. In short, ambient ozone levels were high during both seasons, while CF treatment removed ambient ozone significantly.

The concentration of SO_2 was very low (below 1 ppb) and close to the detection limit of the analytic equipment. The 24 h mean concentration of NO and NO_2 during the two growing seasons never exceeded 5 ppb for either of the two gases. Therefore, the levels of sulphur dioxide and nitrogen oxides were too low to have a substantial effect on the response to ozone in these experiments (Darrall 1989).

At the time of leaf sampling, mature leaves had typical visible ozone injury in NF and, to a greater extent, NF^+ chambers. The visible symptoms mainly consisted of interveinal purple spots and necrosis; some bleaching and yellowing were also visible in certain samples (Fig. 2). Young leaves generally had visible symptoms in the top leaflet in NF^+ chambers, although the young samples collected showed no visible injury.

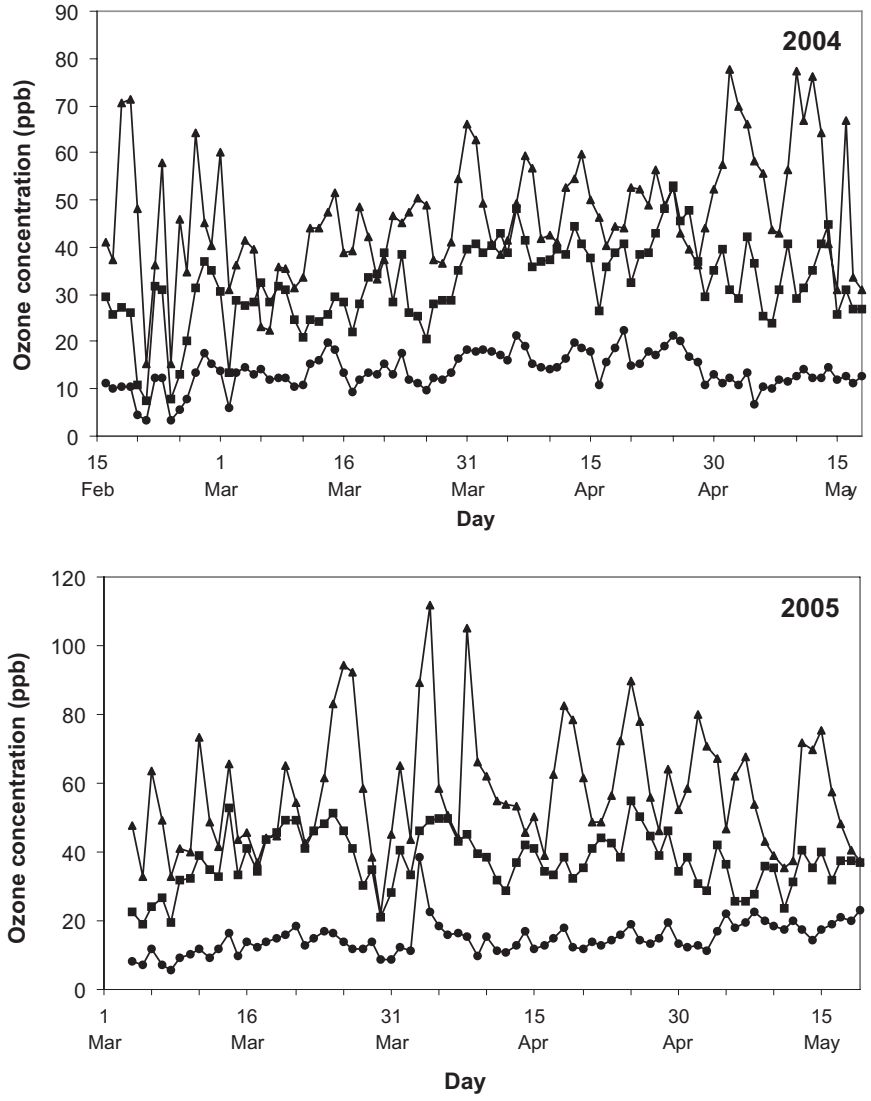

Figure 1. Daily 12 h mean ozone concentration between sunrise and sunset (0800–2000 h) within charcoal-filtered (circles, bottom), non-filtered (squares, middle) and non-filtered plus extra ozone (triangles, top) OTC at Carcaixent (Spain) for the periods from plant emergence to harvest in two crop seasons (16 February–18 May 2004 and 4 March–19 May 2005).

Figure 2. Photographs of mature leaves representative of each treatment (from left to right: charcoal-filtered air, CF; non-filtered air, NF; non-filtered air plus extra ozone, NF^+). Interveinal purple spots are spread throughout the leaf surface in the NF and NF^+ treatments. Arrows indicate necrosis, circles surround bleached spots and asterisks indicate yellowing areas. Yellowing is seen in detail in the amplified area of an NF^+ leaf.

Foliar anatomy

Leaf cross-sections stained with toluidine blue are shown in Fig. 3, which shows the effect of the different treatments on foliar anatomy. In plants exposed to CF, no anomalies were observed in tissue structure (Fig. 3a), which consists of an adaxial epidermis with stomata, a single layer of palisade parenchyma with relatively big cells, vascular bundles devoid of sheath, spongy parenchyma constituting slightly over 50% of the mesophyll volume (which connects directly with the abaxial epidermis, without any specialized intermediary layer) and the abaxial epidermis with a significantly higher stomatal density than the adaxial epidermis, as shown in Table 1. Palisade parenchyma, as well as spongy parenchyma cells, were turgid and attached by an intact middle lamella, and chloroplasts were evenly distributed around the central vacuole (Fig. 3b).

In the NF treatment, young leaves showed no anatomical alterations (Fig. 3c), whereas some were observed in mature leaves (Fig. 3d,e). A degeneration of the middle lamella at specific points in the palisade parenchyma cell walls caused the detachment between adjacent cells at those points. Certain cells had their chloroplasts allocated in the cell centre as a consequence of a decrease in vacuole size. In addition, vacuolar content became denser. These effects were more severe in the spongy parenchyma, where an important proportion of cells acquired irregular shapes as a consequence of the degeneration of their middle lamella and primary cell wall and the loss of vacuole turgor. Chloroplasts became smaller and were located in the cell centre, probably due to tonoplast disintegration. Some cells in the spongy parenchyma were more intensely damaged: they had collapsed and their content was very dense. The loss of cohesion between cells and the decrease in cell volume led to a considerable increase in intercellular space. It was significant that the damage was mainly seen in areas close to the stomata.

In plants grown in ozone-enriched air (NF^+ treatment), the damage described earlier was more intense and appeared earlier in leaf development, because some damage occurred in young leaves (Fig. 3f). In young leaves, cells started to lose cohesion and adopted diverse irregular shapes. The pink-purplish colour acquired with toluidine blue staining and the blurred look of cell walls, particularly at the points of cell detachment, suggested degradation of the primary cell wall and the middle lamella (Krishnamurthy 1988). The central vacuole started to lose turgor; in some cells, chloroplasts were disorganized, a sign of central vacuole disappearance.

In mature leaves from the NF^+ treatment, severe cell damage spread throughout all tissues (Fig 3g–j). Cell collapse reached high proportions in the spongy parenchyma, where most of the cells became star-shaped, and so cell contact was almost completely lost. In certain areas, cells collapsed completely or nearly disappeared. This degradation extended to the palisade parenchyma, where cells were also star-shaped or had collapsed. Densification of the cytoplasm was observed in the damaged cells, possibly as a result of accumulation of phenolic compounds. Even epidermal cells, in the adaxial surface and to a greater extent in the abaxial surface, collapsed, to the point that the epidermis in the most damaged areas became a very thin layer. In addition, there was an interesting finding of deposits that seemed to block the phloem (Fig. 3j).

Table 1. Stomatal density (number of stomata per mm^2) of adaxial and abaxial leaf surfaces measured in the three OTC treatments

No. of stomata per mm^2	CF	NF	NF^+
Adaxial (upper leaf surface)	24.5 ± 1.4	23.0 ± 1.8	22.1 ± 2.3
Abaxial (lower leaf surface)	99.3 ± 6.9**	94.9 ± 7.4**	102.1 ± 6.7**

Asterisks indicate significant differences ($p < 0.01$) between the two leaf surfaces within each treatment. No significant differences were found between treatments.

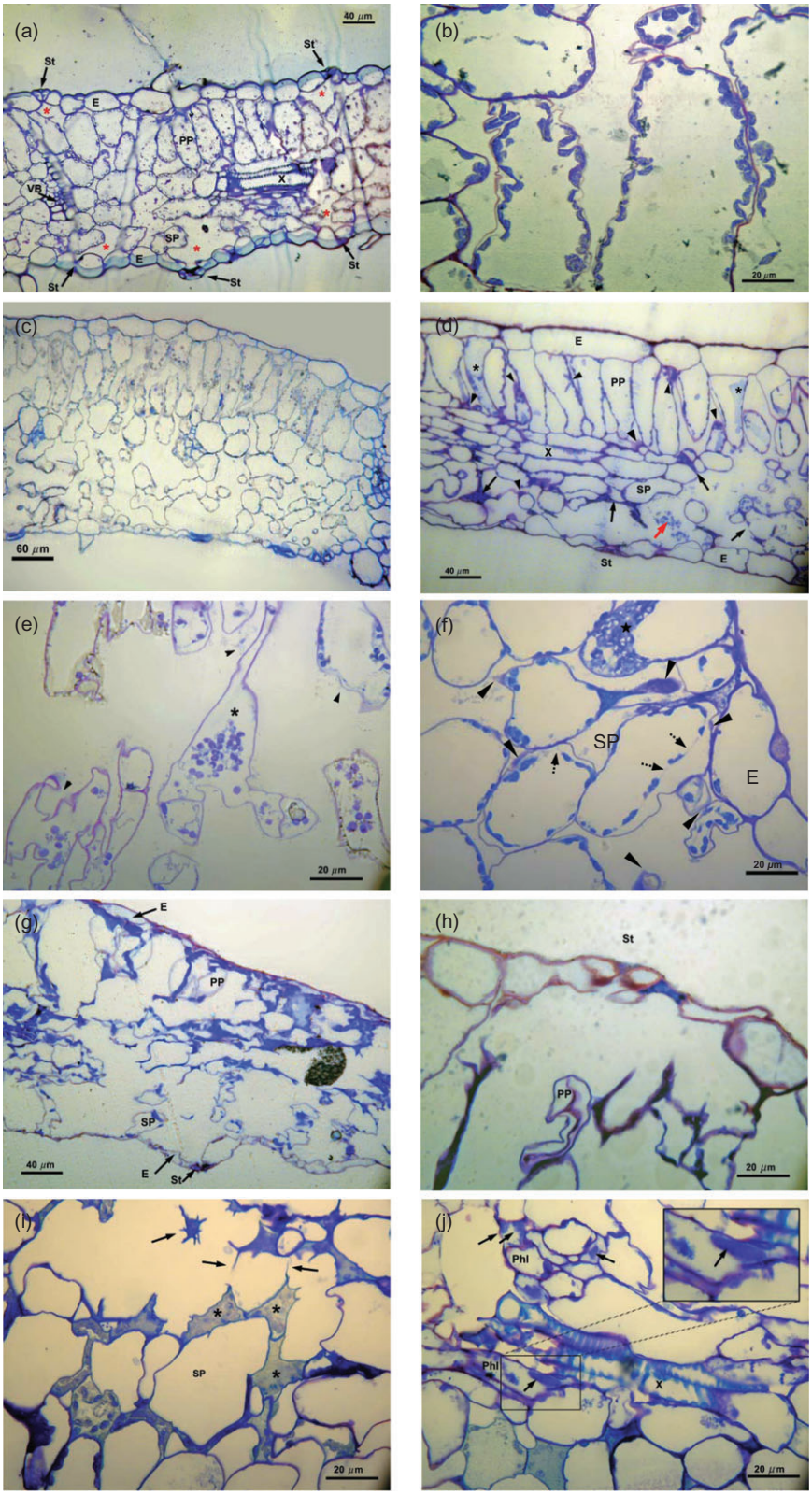

Figure 3. Leaf semi-thin cross sections (1 μm thick) stained with toluidine blue for anatomical observations. (a) General structure of a mature leaf from CF treatment. Arrows indicate the stomata; note the presence of stomata in the adaxial epidermis. Red asterisks show the substomatal cavities. The vascular bundle (VB) is not surrounded by a sheath (see below for other abbreviations); (b) Palisade parenchyma of a mature leaf from CF treatment. Cells are turgid and chloroplasts have a perivacuolar position; (c) Young leaf from NF treatment; (d) Mature leaf from NF treatment. Densification of the vacuolar content is observed (stars). Arrowheads indicate damaged areas of the cell walls, where contact loss between mesophyll cells is possibly initiated; this initial stage of cell damage is more visible in the palisade parenchyma. Damaged cells finally collapse (black arrows) and release their content to the apoplasm (red arrow); these advanced stages of cell damage are observed in the spongy parenchyma; (e) Spongy parenchyma of a mature leaf from NF treatment. Note the irregular cell shape (arrowheads); chloroplasts have become smaller and are dispersed possibly as a consequence of tonoplast disintegration (star); (f) Young leaf from NF^+ treatment. Arrowheads point to damaged cell walls. The vacuole starts to lose turgor (broken arrows) and chloroplasts are disorganized (star); (g) Mature leaf from NF^+ treatment. Cell damage extends throughout the mesophyll and epidermis; (h) Mature leaf from NF^+ treatment. Detail of damaged cells from the palisade parenchyma close to a substomatal cavity; (i) Mature leaf from NF^+ treatment. The process of contact loss between cells and their subsequent size reduction by collapse is shown in detail (arrows). Stars indicate a dense and refringent cytoplasmic content; and (j) Mature leaf from NF^+ treatment. Note the accumulations within the sieve plates (arrows) of a substance, probably callose, obstructing the phloem in the amplified area. Abbreviations: E, Epidermis; Phl, Phloem; PP, Palisade parenchyma; SP, Spongy parenchyma; St, Stomata; VB, Vascular bundle; X, Xylem.

Electron microscopy allowed more detailed observation of the effects described previously in mature samples. The most outstanding ozone effects were found in chloroplasts, which became denser and were completely agglomerated in damaged cells without a central vacuole (Fig. 4b); chloroplasts stored numerous starch grains in comparison with CF samples (Fig. 4a). In highly degenerated chloroplasts, the starch grains had disappeared, leaving an empty lumen and

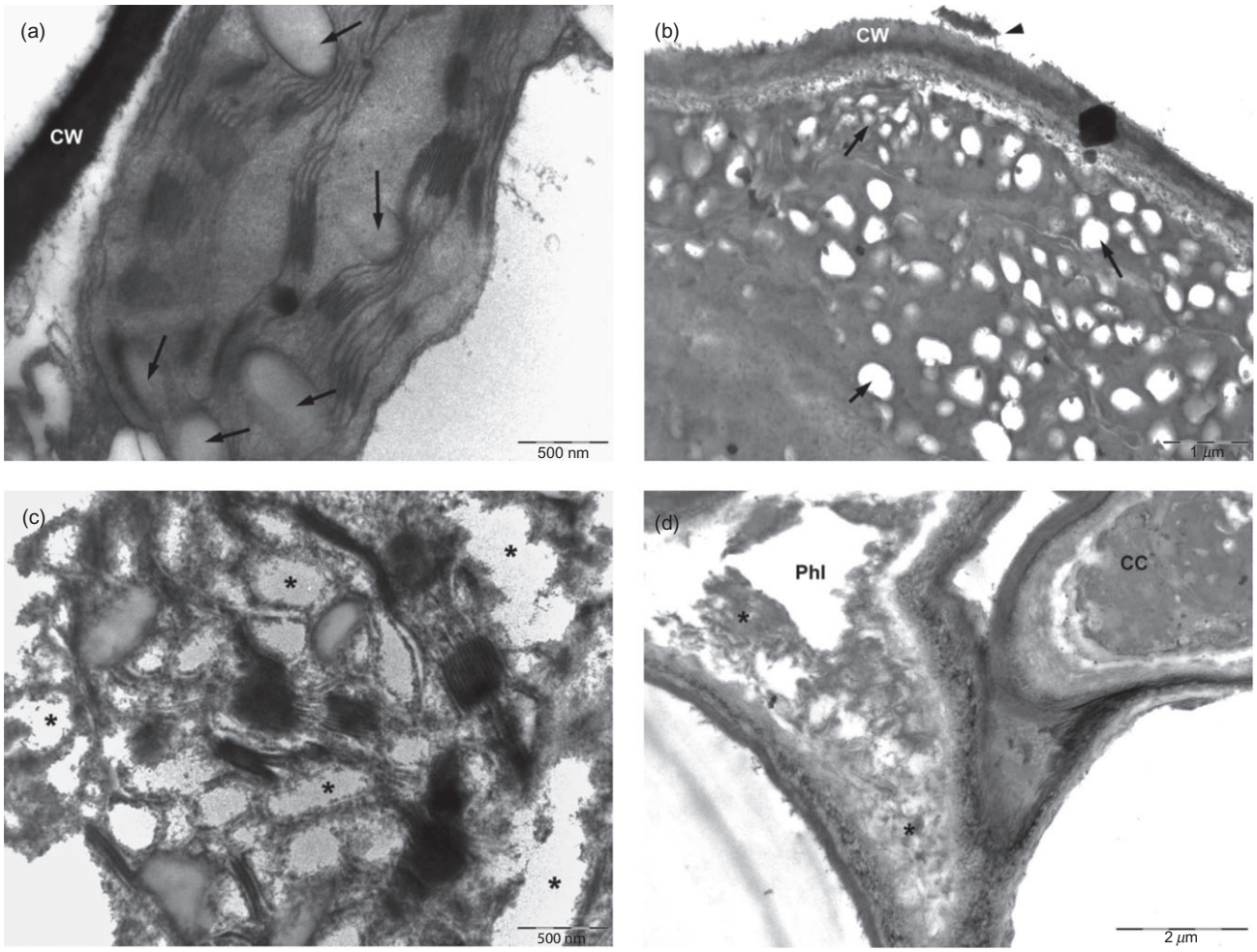

Figure 4. Ultra-thin sections of mature leaves observed by transmission electron microscopy. (a) Cell wall (cw) and chloroplast of a CF sample. Arrows indicate starch grains; (b) Cell wall (cw) and chloroplasts of an NF^+ sample. Arrows indicate some starch grains as an example. Note the detached cell wall fragment (arrowhead); (c) Chloroplast of an NF^+ sample in an advanced state of degeneration. Asterisks indicate the voids left by starch after disappearing; and (d) Phloem (Phl) and companion cell (CC) of a NF^+ sample. Note the significant callose accumulation within the phloem (asterisks).

disrupted thylakoids (Fig. 4c). Cell wall damage was also apparent, as seen in Fig. 4b. The deposits found in the phloem by toluidine blue staining looked electron-translucent under the electron microscope, suggesting that the accumulated substance was callose. Phloem internal width fell considerably because of this accumulation (Fig. 4d).

Callose location

Toluidine blue staining and electron microscopy pointed to the presence of callose in the phloem as a consequence of ozone treatment. To confirm this effect, specific staining with aniline blue was undertaken. Callose was not generally detected in CF samples (Fig. 5a), although small callose deposits in the phloem were found in a very low proportion of the examined sections (data not shown). Callose was detected frequently in the phloem of NF samples (Fig. 5b), and the deposits appeared as blockages. In NF^+ samples (Fig 5c,d), callose was abundant and formed very close deposits, which significantly obstructed the phloem. These observations showed that callose in the phloem increased in a direct relationship with ozone concentration. In NF^+ samples, callose was also found in some cell walls in the palisade parenchyma, specifically in brown-looking cells, which made up the visible symptoms that could be seen on the leaf surface. Occasionally, callose was found in the cell walls of the epidermis adjacent to these parenchymatic cells (Fig. 5d).

Phloem obstruction by callose as a consequence of ozone exposure gave rise to a working hypothesis that ozone had a negative effect on assimilate transport from leaves to sink organs and therefore on tuber yield.

Starch content

Ozone treatment seemed to cause starch accumulation in the leaves, as observed by electron microscopy. To confirm this effect and to determine the precise location of starch, the sections were stained with Lugol. In plants grown under CF air, starch inside the chloroplasts of the palisade and

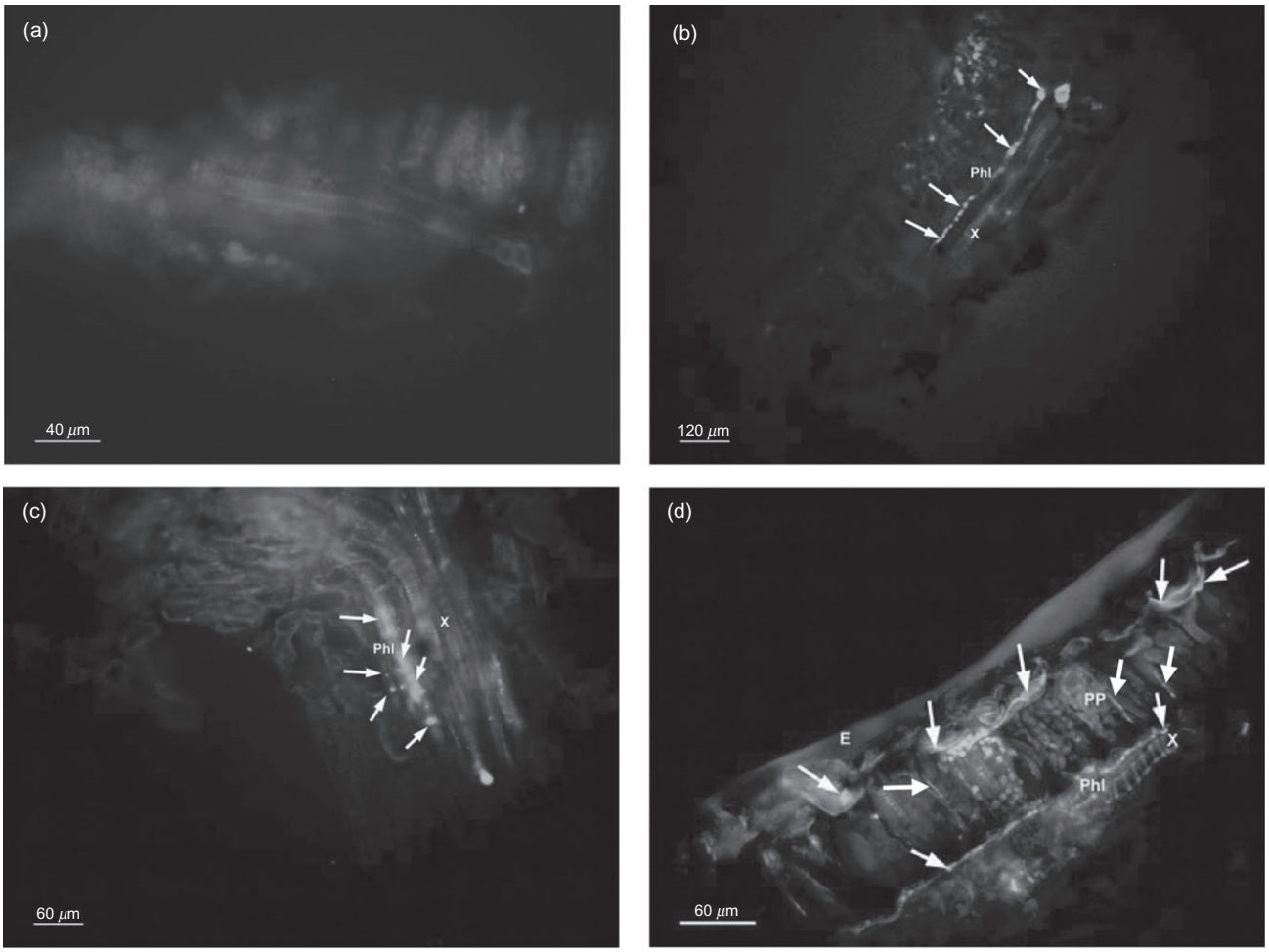

Figure 5. Cross-sections of mature leaves (15 μm thick) stained with aniline blue for callose detection by fluorescence. (a) CF treatment; (b) NF treatment. Arrows indicate callose accumulation within the phloem sieve plates; (c) NF^+ treatment. Arrows indicate callose accumulation as in (b); and (d) NF^+ treatment. Arrows indicate callose location in the walls of palisade parenchyma cells and adjacent epidermis, as well as callose accumulation within the phloem (E: Epidermis, PP: Palisade parenchyma, X: xylem).

spongy parenchymas was barely perceptible (Fig. 6a). When plants were exposed to ambient ozone concentrations (NF treatment), starch content increased, especially in damaged cells, that is, irregularly shaped cells in which the central vacuole had disappeared and chloroplasts were allocated to the cell centre (Fig. 6b). In plants in the NF^+ treatment, starch was abundant and, as in NF samples, was found in damaged cells in the parenchyma (Fig. 6c,d). In contrast, ozone did not affect starch content in the stomata, which were full of starch in the three treatments (Fig. 6a, annexed photograph).

Therefore, Lugol staining demonstrated that ozone caused starch accumulation in parenchymatic damaged cells.

Crop yield

Accumulation of both callose in the phloem and starch in the leaf parenchyma suggested that phloem function was altered and that sugar mobilization from photosynthetic tissues to tubers was affected by ozone. To test this working hypothesis, crop yield inside the OTCs was measured. Crop yield results are summarized in Fig. 7a. Total tuber weight per plant decreased according to ozone concentration. Yield reduction was significant in NF^+ treatment in both years: 42% reduction in 2004 and 29% reduction in 2005, for total tuber production; commercial tuber yield decreased by a similar extent each year (44% and 25% in 2004 and 2005, respectively). Furthermore, NF treatment decreased significantly commercial tuber yield in 2005 (24% yield reduction); in 2004, crop yield in the NF treatment was also lower than CF treatment, although not significantly. Ozone treatments did not affect tuber number per plant (data not shown). In contrast, the effect of ozone was readily apparent in the decrease in average potato weight when only commercial tubers were taken into account. These results showed that ozone affected yield production by decreasing the size of the big tubers. When tuber size was classified into more categories in 2005 (Fig. 7b), the main effect of ozone was effectively found in the biggest tubers (size $\geq$ 60 mm),

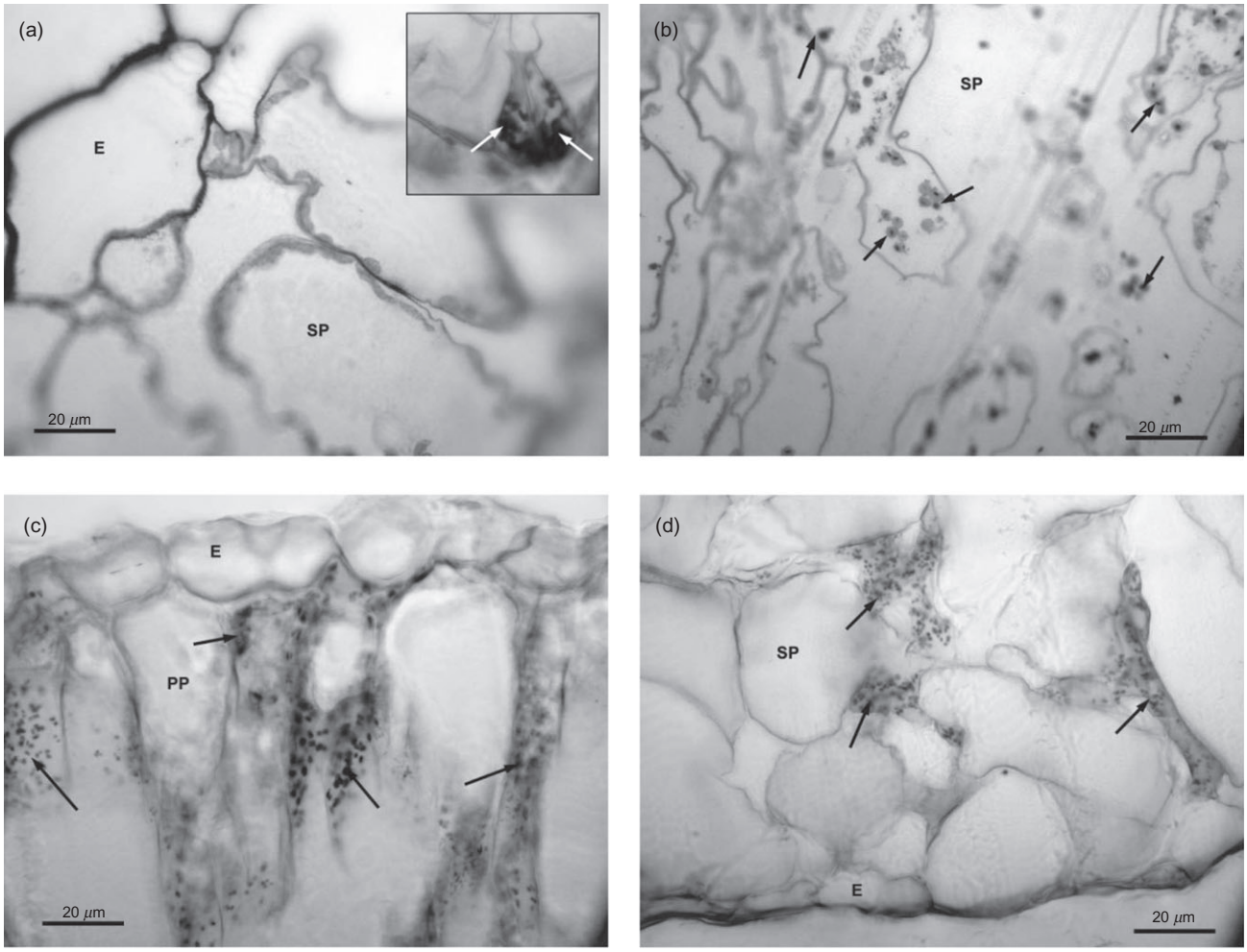

Figure 6. Cross-sections of mature leaves (1 μm thick) stained with Lugol for starch detection. (a) CF treatment. Starch is not appreciable inside the chloroplasts in the parenchyma. The small annexed photograph shows the guard cells of stomata full of starch, which is stained dark blue (arrows); (b) NF treatment. Arrows indicate, as examples, starch grains inside the chloroplasts of parenchymatic damaged cells; (c) NF^+ treatment. Arrows indicate starch grains in damaged cells of the palisade parenchyma; and (d) NF^+ treatment. Arrows indicate starch grains in damaged cells of the spongy parenchyma (E: Epidermis, PP: Palisade parenchyma, SP: Spongy parenchyma).

which fell in number, meaning that their contribution to weight per plant went down. In conclusion, ozone decreased tuber weight, which supported the hypothesis that phloem function was impaired.

DISCUSSION

In the present study, the AOT40 critical level of 3000 ppb h for crops (Fuhrer, Skärby & Ashmore 1997) was exceeded in the ambient air chamber in 2005. In 2004, ambient ozone was close to this value. Significant damage was caused by ozone in both years.

Ozone caused the degeneration of the middle lamella and the cell wall, which led to a loss of cell cohesion and contact at particular points. As a result, the most damaged cells adopted a highly characteristic star-shaped appearance. One consequence of the loss of contact between adjacent cells is the disruption of cell communication through pits and plasmodesmata. Cells finally collapsed and intercellular spaces increased considerably, as observed in a range of species (Günthardt-Goerg *et al.* 1993; Holopainen *et al.* 1996; Reig-Armiñana *et al.* 2004; Bussotti *et al.* 2005; Paoletti *et al.* 2009). A characteristic trait of the action of this pollutant in potato was that damage mainly affected the spongy parenchyma. Because ozone enters the leaf through the stomata (Runeckles 1992), the relationship of fourfold stomatal density on the abaxial surface to that on the adaxial surface probably accounted for higher ozone uptake by the lower leaf surface. An accurate calculation of ozone flux into the leaf would require measurements of stomatal conductance (Pleijel *et al.* 2007). Nevertheless, this goes beyond the scope of our study, which provides an anatomical basis for the differing damage intensities in the two mesophyll layers. This is supported by the observation that the most damaged cells were close to the stomata and probably located on the pathway along which ozone or its

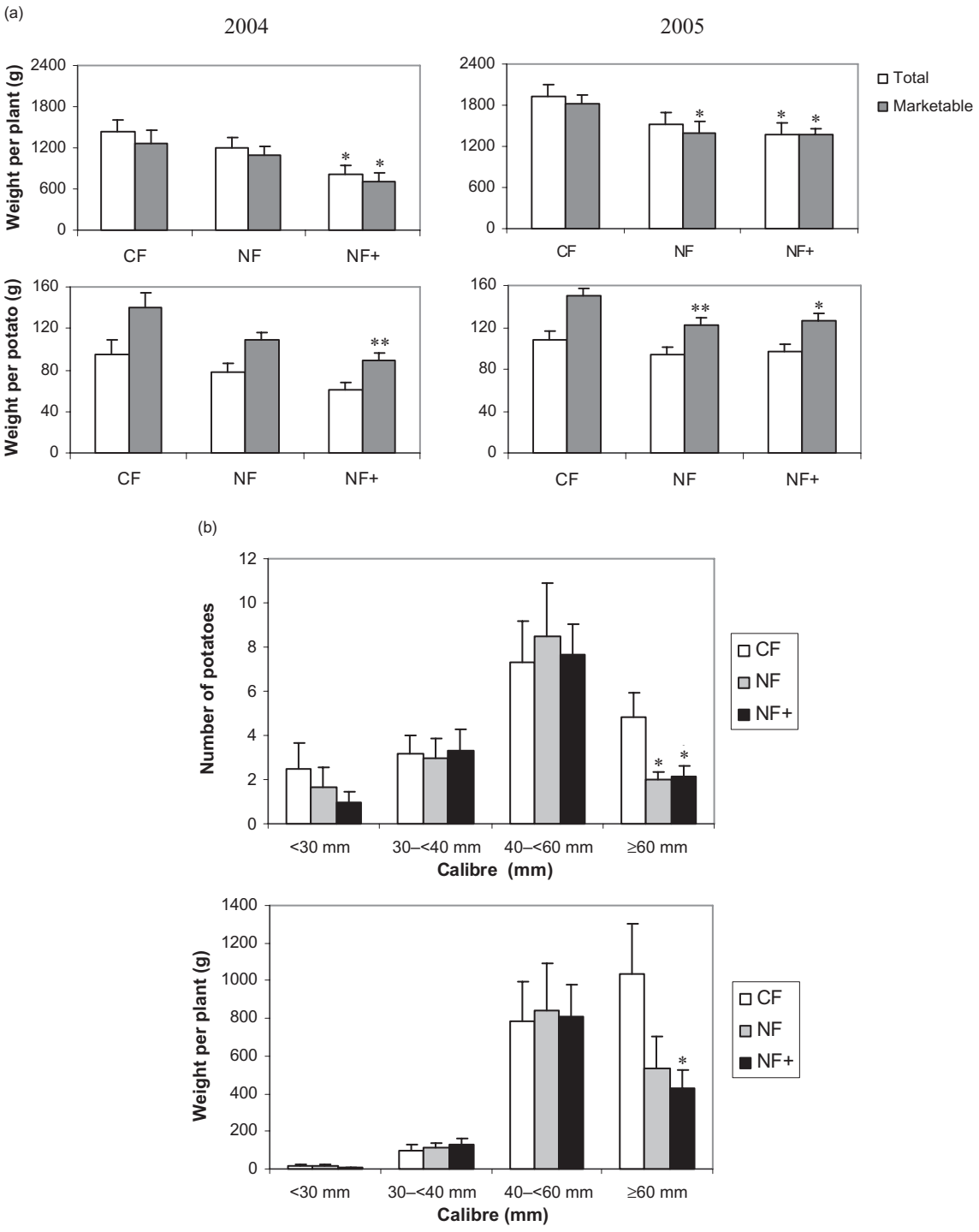

Figure 7. (a) Yield of the two potato crops grown in OTCs (2004, left column; 2005, right column). White bars represent all the tubers, and grey bars represent commercial (marketable) tubers (size ≥ 40 mm). Asterisks indicate significant differences from CF treatment of the corresponding year within each group (total or marketable): $*P < 0.05$, $**$ $P < 0.01$ (post hoc mean comparison performed with LSD test for the variable 'weight per plant' and with Mann-Whitney *U*-test for the variable 'weight per potato'); and (b) Crop yield in 2005 classified according to tuber size (the first two groups are non-commercial size; the following two groups are commercial size). Asterisks indicate significant differences from CF treatment within each size category ($P < 0.05$, post-hoc mean comparison performed with LSD test for the variable 'number of potatoes per plant' and with Mann-Whitney *U*-test for the variable 'weight per plant').

derived reactive species spread. In addition, Faoro & Iriti (2009) found that dead cells after ozone fumigation were mainly located around the stomata.

At the subcellular level, the vacuolar content densified, probably due to phenolic compounds. In particular, the accumulation of condensed tannins in the vacuole has been reported (Günthardt-Goerg *et al.* 2000; Kivimäenpää *et al.* 2001; Matyssek *et al.* 2002), which is considered a protective response against harmful reactive species derived from ozone (Pääkkönen, Gunthardt-Goerg & Holopainen 1998; Saleem *et al.* 2001; Yamaji *et al.* 2003). Subsequently, the tonoplast disintegrated and the perivacuolar arrangement of chloroplasts was lost (Reig-Armiñana *et al.* 2004; Günthardt-Goerg & Vollenweider 2007; Faoro & Iriti 2009; Paoletti *et al.* 2009). Tonoplast damage is attributed to lipid peroxidation by ozone-derived ROS (Rossetti & Medeghini-Bonatti 2001; Biswas *et al.* 2008; Lu *et al.* 2009; Vickers *et al.* 2009). The vacuole disappearance caused a sharp decrease in cell turgor, which probably contributed to the loss of cell contact and finally to cell collapse.

Ozone caused callose deposition in different leaf areas. The deposition of callose in the cell walls of the palisade parenchyma and adaxial epidermis has been described (Gravano *et al.* 2003, 2004; Günthardt-Goerg & Vollenweider 2007). This kind of deposition normally occurs after plant exposure to different abiotic stresses or pathogen attack, in which case callose constitutes a physical barrier that helps to prevent pathogen invasion (Schmelzer 2002; Flors *et al.* 2005; Hardham, Jones & Takemoto 2007). In addition, a remarkable finding of this study was the accumulation of callose inside the phloem. The small and infrequent callose deposits in CF samples are typical of a normal process of senescence. Callose deposits in the phloem increased in plants exposed to ozone in a concentration-dependent manner. Deposition of callose in the phloem after ozone exposure has only been found in birch stems (Matyssek *et al.* 2002), severely limiting assimilate supply and decreasing the root/shoot ratio.

Phloem obstruction by callose hinders the correct loading and circulation of photosynthetic products from leaves for export to sink organs. In potato, developing tubers are an important photoassimilate sink. There is a strong dependence of tuber metabolism on the momentary sucrose supply (Geigenberger & Stitt 2000). In the present study, a significant decrease in crop yield as a result of chronic ozone exposure (14–24% in NF treatment, 29–42% in NF^+ treatment) was found. Total tuber number per plant, which is established at a very early stage of plant development, was not affected by ozone, confirming previous reports (Köllner & Krause 2000; Craigon *et al.* 2002). Yield decrease mainly affected commercial tubers, especially the tubers within the highest size category (≥60 mm). Interestingly, the fact that yield decrease affects the biggest tubers (>50 or >60 mm) has been reported in several other studies (Pell, Pearson & Vinten-Johansen 1988; Craigon *et al.* 2002; Heagle *et al.* 2003). Our results suggest that the progressive obstruction of the phloem by callose affects developing tubers and prevents them from reaching their maximum yield.

The starch accumulation observed in damaged cells, both in NF and NF^+ chambers, seems to indicate impaired assimilate translocation from photosynthetic cells. Starch accumulation in the leaf reaches its maximum at the end of the light period (Geigenberger & Stitt 2000). This might be the reason why CF leaves, collected at midday, had no important starch stores, as observed by Kivimäenpää *et al.* (2001). It has not been possible to determine the mechanisms that lead to sugar immobilization in the form of starch as a response to ozone, although a relationship with the reduced transport capacity of the phloem is not ruled out. Starch accumulation in leaves has been observed under environmental circumstances that cause phloem occlusion, such as phloem bacterial infection (Kim *et al.* 2009), sap-feeding insects (Pirone, Alexander & Lamp 2005), Mg deficiency combined with ozone pollution (Boxler-Baldoma *et al.* 2006) or disease caused by combination of air pollution and mineral deficiencies (Forschner, Schmitt & Wild 1989). In all these studies, authors hypothesized that phloem blockage was responsible for starch accumulation. Furthermore, the study of Kim *et al.* (2009) reported an up-regulation of three key starch biosynthetic genes, which probably led to starch formation from accumulated sucrose. This corroborates the observations of Komor (2000) that, when carbon assimilation exceeds carbon export, the synthesis of starch is up-regulated. Whether such a mechanism is responsible for starch accumulation upon ozone exposure deserves further research, given that ozone impact on carbon assimilation may be dominated by the effects of ozone on carbon transport (Grantz & Farrar 1999).

That ozone-induced phloem obstruction by callose leads to a reduction in below-ground biomass is an important finding. It adds to the already-known negative effects of this pollutant on photosynthesis, resulting in crop yield decrease. This might explain the changes in assimilate partitioning towards above-ground biomass to the detriment of root allocation observed in a number of studies (Miller *et al.* 1998; Grantz & Yang 2000; Wittig *et al.* 2009). Further consequences of a decreased root allocation, such as impairment in the plant's capacity for soil resource acquisition, are a matter of concern (Gerant *et al.* 1996; Fuhrer & Booker 2003; Yamaji *et al.* 2003), and are thus highlighted here. Based on this potential vulnerability, and on the fact that root reduction was found to affect angiosperm trees more dramatically than gymnosperms, Wittig *et al.* (2009) warned that ozone could alter community composition in forests. However, the role of root allocation is barely analysed in the literature about the relationship between ozone and nutrient or water supply. The results of Matyssek *et al.* (2002) on birch demonstrated that the increase in root-to-shoot ratio caused by low fertilization over a high-fertilization regime was almost suppressed by ozone. A similar result was found for two *Plantago major* ozone-resistant lines (Whitfield, Davison & Ashenden 1998). Nutrient availability could also be limited through a decrease in mycorrhizal colonization (Andersen 2003). Effects of ozone-impaired root growth in the capacity of the plant to withstand drought is an almost unexplored field

(Gerant *et al.* 1996), which might help to unravel the complex interaction between the two stressors (Matyssek *et al.* 2006). This is also important for crop management, where nutrient and sometimes water levels can be regulated.

In conclusion, the study of the effects of ozone at the anatomical level in potato have resulted in novel findings. In particular, phloem obstruction by callose and starch accumulation in mesophyll cells of the leaves explained the decreases in tuber yield found even at ambient concentrations of this pollutant. This mechanism might underlie the reductions in below-ground biomass or root-to-shoot ratio found in many other species upon ozone exposure. Further research aimed at confirming this will be relevant.

ACKNOWLEDGMENTS

The authors thank Prof Secundino del Valle (Valencia University, Spain) for his helpful comments. We are also grateful to Mr Duncan Gates for revising the English style of the text. AAF was supported by a grant from the Generalitat Valenciana's FPI programme (Government of Valencia, Spain).

REFERENCES

Andersen C.P. (2003) Source-sink balance and carbon allocation below ground in plants exposed to ozone. *New Phytologist* **157,** 213–228.

Asensi-Fabado A., Carrasco-Rodríguez J.L., Gómez-García C.J. & Valle-Tascón S. (2008) Long-term ozone exposure of potato: free radical content and leaf injury analysed by Q-band ESR spectroscopy and image analysis. *Free Radical Research* **42,** 105–113.

Biswas D.K., Xu H., Li Y.G., Sun J.Z., Wang X.Z., Han X.G. & Jiang G.M. (2008) Genotypic differences in leaf biochemical, physiological and growth responses to ozone in 20 winter wheat cultivars released over the past 60 years. *Global Change Biology* **14,** 46–59.

Boxler-Baldoma C., Lutz C., Heumann H.G. & Siefermann-Harms D. (2006) Structural changes in the vascular bundles of light-exposed and shaded spruce needles suffering from mg deficiency and ozone pollution. *Journal of Plant Physiology* **163,** 195–205.

Bussotti F., Gravano E., Grossoni P., Tani C. & Mori B. (2003) Ultrastructural responses of a Mediterranean evergreen shrub (*Arbutus unedo* L.) fumigated with ozone. In *Air Pollution, Global Change and Forests in the New Millennium. Developments in Environmental Science, 3* (eds D.F. Karnosky, K.E. Percy, A.H. Chappelka, C.J. Simpson & J. Pikkarainen), pp. 269–276. Elsevier Science Ltd, Oxford, UK.

Bussotti F., Agati G., Desotgiu R., Matteini P. & Tani C. (2005) Ozone foliar symptoms in woody plant species assessed with ultrastructural and fluorescence analysis. *New Phytologist* **166,** 941–955.

Carrasco-Rodríguez J.L. & Del Valle-Tascón S. (2001) Impact of elevated ozone on chlorophyll *a* fluorescence in field-grown oat (*Avena sativa*). *Environmental and Experimental Botany* **45,** 133–142.

Clarke B.B., Greenhalgh-Weidman B. & Brennan E.G. (1990) An assessment of the impact of ambient ozone on field-grown crops in New Jersey using the EDU method: part 1- white potato (*Solanum tuberosum*). *Environmental Pollution* **66,** 351–360.

Craigon J., Fangmeier A., Jones M., Donnelly A., Bindi M., DeTemmerman L., Persson K. & Ojanpera K. (2002) Growth and marketable-yield responses of potato to increased CO_2 and ozone. *European Journal of Agronomy* **17,** 273–289.

Darrall N.M. (1989) The effect of air pollutants on physiological processes in plants. *Plant, Cell & Environment* **12,** 1–30.

Derwent R.G., Stevenson D.S., Collins W.J. & Johnson C.E. (2004) Intercontinental transport and the origins of the ozone observed at surface sites in Europe. *Atmospheric Environment* **38,** 1891–1901.

FAO (2009) Website of the Food and Agriculture Organization of the United Nations. Available from URL: http://www.fao.org

Faoro F. & Iriti M. (2009) Plant cell death and cellular alterations induced by ozone: key studies in Mediterranean conditions. *Environmental Pollution* **157,** 1470–1477.

Fiscus E.L., Booker F.L. & Burkey K.O. (2005) Crop responses to ozone: uptake, modes of action, carbon assimilation and partitioning. *Plant, Cell & Environment* **28,** 997–1011.

Flors V., Ton J., Jakab G. & Mauch-Mani B. (2005) Abscisic acid and callose: team players in defence against pathogens? *Journal of Phytopathology* **153,** 377–383.

Forschner W., Schmitt V. & Wild A. (1989) Investigations on the starch content and ultrastructure of spruce needles relative to the occurrence of novel forest decline. *Botanica Acta* **102,** 208–221.

Fuhrer J. & Booker F.L. (2003) Ecological issues related to ozone: agricultural issues. *Environment International* **29,** 141–154.

Fuhrer J., Skärby L. & Ashmore M.R. (1997) Critical levels for ozone: effects on vegetation in Europe. *Environmental Pollution* **97,** 91–106.

Fumagalli I., Gimeno B.S., Velissariou D., De Temmerman L. & Mills G. (2001) Evidence of ozone-induced adverse effects on crops in the Mediterranean region. *Atmospheric Environment* **35,** 2583–2587.

Geigenberger P. & Stitt M. (2000) Diurnal changes in sucrose, nucleotides, starch synthesis and *AGPS* transcript in growing potato tubers that are suppressed by decreased expression of sucrose phosphate synthase. *The Plant Journal* **23,** 795–806.

Gerant D., Podor M., Grieu P., Afif D., Cornu S., Morabito D., Banvoy J., Robin C. & Dizengremel P. (1996) Carbon metabolism enzyme activities and carbon partitioning in Pinus halepensis Mill exposed to mild drought and ozone. *Journal of Plant Physiology* **148,** 142–147.

Grantz D.A. & Farrar J.F. (1999) Acute exposure to ozone inhibits rapid carbon translocation from source leaves of pima cotton. *Journal of Experimental Botany* **50,** 1253–1262.

Grantz D.A. & Yang S. (2000) Ozone impacts on allometry and root hydraulic conductance are not mediated by source limitation nor developmental age. *Journal of Experimental Botany* **51,** 919–927.

Gravano E., Giulietti V., Desotgiu R., Bussotti F., Grossoni P., Gerosa G. & Tani C. (2003) Foliar response of an *Ailanthus altissima* clone in two sites with different levels of ozone-pollution. *Environmental Pollution* **121,** 137–146.

Gravano E., Bussotti F., Strasser R.J., Schaub M., Novak K., Skelly J. & Tani C. (2004) Ozone symptoms in leaves of woody plants in open-top chambers: ultrastructural and physiological characteristics. *Physiologia Plantarum* **121,** 620–633.

Guidi L., Degl'Innocenti E. & Soldatini G.F. (2002) Assimilation of CO_2, enzyme activation and photosynthetic electron transport in bean leaves, as affected by high light and ozone. *New Phytologist* **156,** 377–388.

Günthardt-Goerg M.S. & Vollenweider P. (2007) Linking stress with macroscopic and microscopic leaf response in trees: new diagnostic perspectives. *Environmental Pollution* **147,** 467–488.

Günthardt-Goerg M.S., Matyssek R., Scheidegger C. & Keller T. (1993) Differentiation and structural decline in the leaves and bark of birch (*Betula pendula*) under low ozone concentrations. *Trees-Structure and Function* **7,** 104–114.

Günthardt-Goerg M.S., McQuattie C.J., Maurer S. & Frey B. (2000) Visible and microscopic injury in leaves of five deciduous tree species related to current critical ozone levels. *Environmental Pollution* **109,** 489–500.

Hardham A.R., Jones D.A. & Takemoto D. (2007) Cytoskeleton and cell wall function in penetration resistance. *Current Opinion in Plant Biology* **10,** 342–348.

Heagle A.S. (1989) Ozone and crop yield. *Annual Review of Phytopathology* **27,** 397–423.

Heagle A.S., Miller J.E. & Pursley W.A. (2003) Growth and yield responses of potato to mixtures of carbon dioxide and ozone. *Journal of Environmental Quality* **32,** 1603–1610.

Holopainen T., Anttonen S., Palomaki V., Kainulainen P. & Holopainen J.K. (1996) Needle ultrastructure and starch content in Scots pine and Norway spruce after ozone fumigation. *Canadian Journal of Botany-Revue Canadienne De Botanique* **74,** 67–76.

Kärenlampi L. & Skärby L. (1996) Critical levels of ozone in Europe: testing and finalizing the concepts. In *UN-ECE Workshops Reports* (eds L. Kärenlampi & L. Skärby), p. 363. University of Kuopio, Kuopio, Finland.

Kim J.S., Sagaram U.S., Burns J.K., Li J.L. & Wang N. (2009) Response of sweet orange (*Citrus sinensis*) to 'candidatus *Liberibacter asiaticus*' infection: microscopy and microarray analyses. *Phytopathology* **99,** 50–57.

Kivimäenpää M., Sutinen S., Medin E.L., Karlsson P.E. & Sellden G. (2001) Diurnal changes in microscopic structures of mesophyll cells of Norway spruce, *Picea abies* (L.) Karst., and the effects of ozone and drought. *Annals of Botany* **88,** 119–130.

Köllner B. & Krause G.H.M. (2000) Changes in carbohydrates, leaf pigments and yield in potatoes induced by different ozone exposure regimes. *Agriculture, Ecosystems and Environment* **78,** 149–158.

Komor E. (2000) Source physiology and assimilate transport: the interaction of sucrose metabolism, starch storage and phloem export in source leaves and the effects on sugar status in phloem. *Australian Journal of Plant Physiology* **27,** 497–505.

Krishnamurthy K.V. (1988) *Methods in Plant Histochemistry*. S Viswanathan Press, Madras, India.

Krupa S., McGrath M.T., Andersen C.P., Booker F.L., Burkey K.O., Chappelka A.H., Chevone B.I., Pell E.J. & Zilinskas B.A. (2001) Ambient ozone and plant health. *Plant Disease* **85,** 4–12.

Kuik O.J., Helming J.F.M., Dorland C. & Spaninks F.A. (2000) The economic benefits to agriculture of a reduction of low level ozone pollution in the Netherlands. *European Review of Agricultural Economics* **27,** 75–90.

Langebartels C., Schraudner M., Heller W., Ernst W. & Sandermann H. (2002) Oxidative stress and defense reactions in plants exposed to air pollutants and UV-B radiation. In *Oxidative Stress in Plants* (eds D. Inzé & M. Van Montagu), pp. 105–135. Taylor and Francis, London, UK.

Lu T., He X.Y., Chen W., Yan K. & Zhao T.H. (2009) Effects of elevated O-3 and/or elevated Co2 on lipid peroxidation and antioxidant systems in *Ginkgo biloba* leaves. *Bulletin of Environmental Contamination and Toxicology* **83,** 92–96.

Matyssek R., Günthardt-Goerg M.S., Maurer S. & Christ R. (2002) Tissue structure and respiration of stems of *Betula pendula* under contrasting ozone exposure and nutrition. *Trees-Structure and Function* **16,** 375–385.

Matyssek R., Le Thiec D., Low M., Dizengremel P., Nunn A.J. & Haberle K.H. (2006) Interactions between drought and O-3 stress in forest trees. *Plant Biology* **8,** 11–17.

Millán M., Sanz M.J., Salvador R. & Mantilla E. (2002) Atmospheric dynamics and ozone cycles related to nitrogen deposition in the western Mediterranean. *Environmental Pollution* **118,** 167–186.

Miller J.E., Heagle A.S. & Pursley W.A. (1998) Influence of ozone stress on soybean response to carbon dioxide enrichment. II. Biomass and development. *Crop Science* **38,** 122–128.

Miyake H., Matsumura H., Fujinuma Y. & Totsuka T. (1989) Effects of low concentrations of ozone on the fine structure of radish leaves. *New Phytologist* **111,** 187–195.

Morgan P.B., Ainsworth E.A. & Long S.P. (2003) How does elevated ozone impact soybean? A meta-analysis of photosynthesis, growth and yield. *Plant, Cell & Environment* **26,** 1317–1328.

Oksanen E., Häikiö E., Sober J. & Karnosky D.F. (2003) Ozone-induced H_2O_2 accumulation in field-grown aspen and birch is linked to foliar ultrastructure and peroxisomal activity. *New Phytologist* **161,** 791–799.

Pääkkönen E., Holopainen T. & Kärenlampi L. (1995) Ageing-related anatomical and ultrastructural changes in leaves of birch (*Betula pendula* Roth.) clones as affected by low ozone exposure. *Annals of Botany* **75,** 285–294.

Pääkkönen E., Gunthardt-Goerg M.S. & Holopainen T. (1998) Responses of leaf processes in a sensitive birch (*Betula pendula* Roth) clone to ozone combined with drought. *Annals of Botany* **82,** 49–59.

Paoletti E., Contran N., Bernasconi P., Gunthardt-Goerg M.S. & Vollenweider P. (2009) Structural and physiological responses to ozone in manna ash (*Fraxinus ornus* L.) leaves of seedlings and mature trees under controlled and ambient conditions. *Science of the Total Environment* **407,** 1631–1643.

Pell E.J., Pearson N.S. & Vinten-Johansen C. (1988) Qualitative and quantitative effects of ozone and/or sulfur dioxide on field-grown potato plants. *Environmental Pollution* **53,** 171–186.

Pell E.J., Eckhardt N. & Eniyedi A.J. (1992) Timing of ozone stress and resulting status of ribulose biphosphate carboxylase/oxygenase and associated net photosynthesis. *New Phytologist* **120,** 397–408.

Pirone C.L., Alexander L.C. & Lamp W.O. (2005) Patterns of starch accumulation in alfalfa subsequent to potato leafhopper (*Homoptera cicadellidae*) injury. *Environmental Entomology* **34,** 199–204.

Pleijel H., Danielsson H., Emberson L., Ashmore M.R. & Mills G. (2007) Ozone risk assessment for agricultural crops in Europe: further development of stomatal flux and flux-response relationships for European wheat and potato. *Atmospheric Environment* **41,** 3022–3040.

Prather M., Ehhalt D., Dentener F., Berntsen T. & Smith S.J. (2001) Atmospheric chemistry and greenhouse gases. In *Climate Change 2001: the Scientific Basis Contribution of Working Group I to the Third Assessment Report of the Intergovernmental Panel on Climate Change* (eds J.T. Houghton, Y. Ding, D.J. Griggs, M. Noguer, P.J. Van der Linden, X. Dai, K. Maskell & C.A. Johnson), pp. 239–287. Cambridge University Press, Cambridge, UK.

Reig-Armiñana J., Calatayud V., Cerveró J., García-Breijo F.J., Ibars A. & Sanz M.J. (2004) Effects of ozone on the foliar histology of the mastic plant (*Pistacia Lentiscus* L.). *Environmental Pollution* **132,** 321–331.

Rossetti S. & Medeghini-Bonatti P. (2001) In situ histochemical monitoring of ozone- and TMV-induced reactive oxygen species in tobacco leaves. *Plant Physiology and Biochemistry* **39,** 433–442.

Runeckles V.C. (1992) Uptake of ozone by vegetation. In *Surface Level Ozone Exposures and Their Effect on Vegetation* (ed. A.S. Lefohn), pp. 157–188. Lewis Publishers, Chelsea, MI, USA.

Runeckles V.C. & Chevone B.I. (1992) Crop responses to ozone. In *Surface Level Ozone Exposures and Their Effects on Vegetation* (ed. A.S. Lefohn), pp. 189–270. Lewis Publishers, Chelsea, MI, USA.

Saleem A., Loponen J., Pihlaja K. & Oksanen E. (2001) Effects of long-term open-field ozone exposure on leaf phenolics of European silver birch (*Betula pendula* Roth). *Journal of Chemical Ecology* **27,** 1049–1062.

Schmelzer E. (2002) Cell polarization, a crucial process in fungal defence. *Trends in Plant Science* **7,** 411–415.

U.S. EPA (2006) *Air Quality Criteria for Ozone and Related Photochemical Oxidants*. U.S. Environmental Protection Agency, Washington, DC, USA. EPA/600/R-05/004aF-cF.

Vickers C.E., Possell M., Cojocariu C.I., Velikova V.B., Laothawornkitkul J., Ryan A., Mullineaux P.M. & Hewitt C.N. (2009) Isoprene synthesis protects transgenic tobacco plants from oxidative stress. *Plant, Cell & Environment* **32,** 520–531.

Vingarzan R. (2004) A review of surface O_3 background levels and trends. *Atmospheric Environment* **38,** 3431–3442.

Violini G., Maffi D., Conti G.G., Faoro F. & Tornaghi R. (1992) Damage by ambient ozone to bean leaves. Histological, histochemical and ultrastructural observations. *Rivista di Patologia Vegetale* **2,** 91–110.

Wang X.P. & Mauzerall D.L. (2004) Characterizing distributions of surface ozone and its impact on grain production in China, Japan and South Korea: 1990 and 2020. *Atmospheric Environment* **38,** 4383–4402.

Whitfield C.P., Davison A.W. & Ashenden T.W. (1998) The effects of nutrient limitation on the response of Plantago major to ozone. *New Phytologist* **140,** 219–230.

Wittig V.E., Ainsworth E.A., Naidu S.L., Karnosky D.F. & Long S.P. (2009) Quantifying the impact of current and future tropospheric ozone on tree biomass, growth, physiology and biochemistry: a quantitative meta-analysis. *Global Change Biology* **15,** 396–424.

Yamaji K., Julkunen-Tiitto R., Rousi M., Freiwald V. & Oksanen E. (2003) Ozone exposure over two growing seasons alters root-to-shoot ratio and chemical composition of birch (*Betula pendula* Roth). *Global Change Biology* **9,** 1363–1377.